Mutual Linearity of Nonequilibrium Network Currents

Pedro E. Harunari[1,*] Sara Dal Cengio,[2] Vivien Lecomte,[2] and Matteo Polettini[3]

[1]*Department of Physics and Materials Science, University of Luxembourg, Campus Limpertsberg,*
162a avenue de la Faïencerie L-1511, Luxembourg
[2]*Laboratoire Interdisciplinaire de Physique, University of Grenoble, France*
[3]*Via Gaspare Nadi 4, 40139 Bologna (BO), Italy*

For continuous-time Markov chains and open unimolecular chemical reaction networks, we prove that any two stationary currents are linearly related upon perturbations of a single edge's transition rates, arbitrarily far from equilibrium. We extend the result to nonstationary currents in the frequency domain, provide and discuss an explicit expression for the current-current susceptibility in terms of the network topology, and discuss possible generalizations. In practical scenarios, the mutual linearity relation has predictive power and can be used as a tool for inference or model proof testing.

Nonequilibrium thermodynamics is usually framed as a theory of the response of observable currents to driving forces and is often predicated on its ability to describe nonlinear effects far from equilibrium, i.e., in the absence of detailed balance. It has historical roots in such results as Einstein's relation [1], Nyquist's formula [2], the Green-Kubo and the Casimir-Onsager reciprocal relations [3,4], all derived under the assumption that the (mean) currents are linearly related to the driving forces. Beyond the linear regime, cornerstone results are the fluctuation relations [5,6], which allow one to derive higher-order response and reciprocity relations [7,8]. Nonlinearity can lead to interesting phenomena such as relaxation slowdown [9] or negative response due to the internal activity in the system [10,11] associated with complex behavior, e.g., in biological systems (homeostasis, bifurcations, limit cycles, etc.).

All these results regard the response of currents to a variation of the driving forces. However, if we take currents as the fundamental observables, it makes sense to bypass forces and establish relations among the currents themselves. This is also motivated by phenomenological considerations. Think, for example, of the mercury-in-glass thermometer once in use: it is only when the fluid stops moving that we read our body temperature, but on the other hand the thermometer scale was set by Celsius and coevals by stabilization with the universal phenomenon of heat flow between the melting ice and the boiling water at sea level [12,13]. Thus, the calibration of forces depends on observations about currents.

A ubiquitous framework to study fluctuations in stochastic phenomena in physics (especially at the intersection with chemistry and biology) is that of continuous-time

Markov chains [14–17]. Here, possible system configurations are represented as vertices in a network (or graph) $\mathcal{G}$ connected by edges. Transitions between vertices along an edge, in either direction, occur at rates due to the interaction of the system with the environment. Network currents then count the net number of such events, and they can be used as building blocks for all relevant thermodynamic quantities such as heat, work, entropy production, etc. Heat flow is defined as a linear combination of network currents multiplied by the energy they displace; entropy production is a linear combination of heat flows multiplied by their conjugate thermodynamic potentials. In the long-time limit, network currents become stationary and satisfy Kirchhoff's current law, which is granted conservation of some underlying quantity (be it charges, matter, or, as in our case, probability). This purely topological constraint implies that not all network currents are independent. In a unicyclic network, all edges in the cycle share the same stationary current, independently of the rates. For multicyclic networks, Kirchhoff's current law alone does not constrain all of the currents, and since currents typically depend nonlinearly on the transition rates, there is no *a priori* reason to believe they should satisfy simple relations among themselves.

In fact, in this contribution we show that all stationary currents are linearly related with respect to variations of the forward and backward rates along one edge.

We consider a continuous-time Markov chain over a finite network consisting of $|\mathcal{X}|$ vertices $\mathrm{x} \in \mathcal{X}$ connected by $|\mathcal{E}|$ edges $e \in \mathcal{E}$, to which we assign an arbitrary orientation. We denote by $\pm e$ transitions along an edge e in the direction either parallel or antiparallel to the edge's orientation, from source vertex $\mathrm{s}(\pm e)$ to target vertex $\mathrm{s}(\mp e)$. Transitions occur at time-independent probability rates $r_{\pm e}$. The only assumption we make on the rates is that the network is irreducible, that is, that there exists a directed

*Contact author: pedro.harunari@uni.lu

path of nonvanishing probability between any two vertices. In particular, the so-called cycle affinities [18] playing the role of fundamental driving forces can take arbitrary values.

Let $p_{\mathrm{x}}(t)$ be the probability to be in state x at time t. Vector $\mathbf{p}(t) = (p_{\mathrm{x}})_{\mathrm{x} \in \mathcal{X}}$ evolves via the master equation $\partial_t \mathbf{p}(t) = \mathbf{R}\mathbf{p}(t)$, where $\mathbf{R}$ is the rate matrix with non-diagonal elements $[\mathbf{R}]_{\mathrm{s}(\mp e), \mathrm{s}(\pm e)} = r_{\pm e}$. The normalized null vector of $\mathbf{R}$ is the unique stationary distribution $\boldsymbol{\pi}$. The stationary currents are defined as

$$J_e := r_{+e}\pi_{\mathrm{s}(+e)} - r_{-e}\pi_{\mathrm{s}(-e)}. \tag{1}$$

We promote one particular edge i as the input edge on the assumption it is not a bridge—an edge whose removal disconnects the graph—and study the dependence of all other stationary (output) currents on its transition rates $\boldsymbol{r}_i = (r_{+i}, r_{-i})$, while leaving all other rates unchanged.

In general, all $J_e(\boldsymbol{r}_i)$ are nonlinear functions of $\boldsymbol{r}_i$ (see Fig. 1, top inset). In fact, as a spinoff result, we prove in Sec. I of the Supplemental Material [19] that they are upper- and lower-bounded. Here, we investigate the mutual relations among the currents themselves. Inspired by Ref. [20], we exploit a property of the rate matrix to obtain the response of stationary currents to changes of r_{+i}, r_{-i}, or both simultaneously. Let $\mathbf{R}_{\mathrm{s}(+i)}$ be defined as $\mathbf{R}$ with row $\mathrm{s}(+i)$ replaced by an array of ones; then the product $\mathbf{R}_{\mathrm{s}(+i)}\boldsymbol{\pi}$ yields a vector of zeros but for value 1 at position $\mathrm{s}(+i)$. This owns to the normalization $\boldsymbol{\pi} \cdot \mathbf{1} = 1$, with $\mathbf{1}$ a vector with all unit entries and $\cdot$ the Euclidean scalar product. Since, in contrast to the rate matrix, $\mathbf{R}_{\mathrm{s}(+i)}$ is invertible (see Sec. II of the Supplemental Material [19] for an alternative proof to Refs. [20,21]), the response of the stationary distribution can be obtained by $\partial_{r_{\pm i}}\boldsymbol{\pi} = -\mathbf{R}_{\mathrm{s}(+i)}^{-1}(\partial_{r_{\pm i}}\mathbf{R}_{\mathrm{s}(+i)})\boldsymbol{\pi}$. This relation can be used to obtain the responses $\partial_{r_{\pm i}}J_i$ and $\partial_{r_{\pm i}}J_e$. Their full-extent expressions can be found in Sec. III of the Supplemental Material [19], but the relevant piece of information is that their ratio satisfies $(\partial_{r_{\pm i}}J_e)/(\partial_{r_{\pm i}}J_i) = \lambda_{e \leftarrow i}^1$ with $\lambda_{e \leftarrow i}^1$ independent of $\boldsymbol{r}_i$. Since a gradient fixes the field up to a potential, this yields the linear relation

$$J_e(\boldsymbol{r}_i) = \lambda_{e \leftarrow i}^0 + \lambda_{e \leftarrow i}^1 J_i(\boldsymbol{r}_i), \tag{2}$$

with $\lambda_{e \leftarrow i}^0$ also independent of $\boldsymbol{r}_i$. If i is a bridge $[J_i(\boldsymbol{r}_i) = 0 \ \forall \ \boldsymbol{r}_i]$ the above formula does not hold, and $\lambda_{e \leftarrow i}^1$ diverges.

Equation (2) is our main result: control of the rates of an input edge causes a linear response in any stationary current with respect to the input one. The result is illustrated in Fig. 1. The affine coefficient $\lambda_{e \leftarrow i}^0 = J_e(\mathbf{0})$ can easily be interpreted as the current through edge e when the input rates are set to values such that the input current vanishes, a condition called stalling already shown to be relevant in traditional linear-regime theory [22]. The linear coefficient
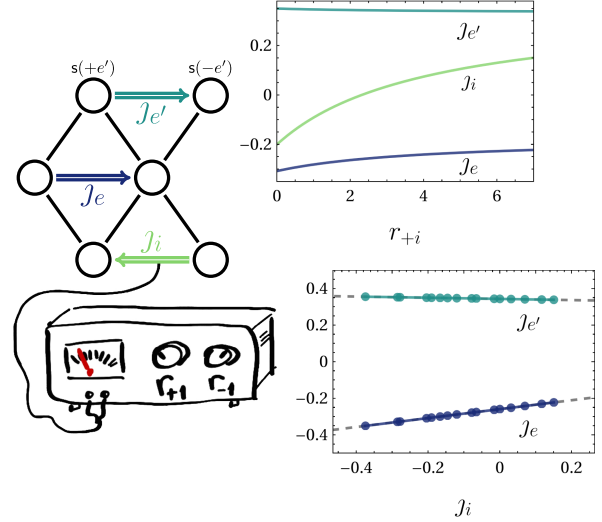

FIG. 1. Scheme of the control over the input current J_i and its linear relation to J_e and $J_{e'}$ in a network. Top inset: plot of the nonlinear relation of all three currents in terms of r_{+i}, with $r_{-i} = 1$. Bottom inset: plot of the two output currents' linear relation with respect to the input one, with dashed lines obtained by Eq. (2) and dots representing values of $r_{\pm i} \in [0, 3]$ (see details in Sec. VIII of the Supplemental Material [19]).

$\lambda_{e \leftarrow i}^1$ can be interpreted as a current-current edge susceptibility (from now on, simply susceptibility); we will derive and discuss an explicit expression later on.

As a generalization, consider macroscopic currents supported by many edges, $\mathcal{J}_E := \sum_{e \in E} c_e J_e$ for constant coefficients c_e. Let $\Lambda_{E \leftarrow i}^0 = \sum_{e \in E} c_e \lambda_{e \leftarrow i}^0$ and $\Lambda_{E \leftarrow i}^1 = \sum_{e \in E} c_e \lambda_{e \leftarrow i}^1$. Because $\mathcal{J}_E(\boldsymbol{r}_i) = \Lambda_{E \leftarrow i}^0 + \Lambda_{E \leftarrow i}^1 J_i(\boldsymbol{r}_i)$, we find that any two macroscopic currents are mutually related by

$$\mathcal{J}_{E'}(\boldsymbol{r}_i) = \left(\Lambda_{E' \leftarrow i}^0 - \frac{\Lambda_{E' \leftarrow i}^1}{\Lambda_{E \leftarrow i}^1}\Lambda_{E \leftarrow i}^0\right) + \frac{\Lambda_{E' \leftarrow i}^1}{\Lambda_{E \leftarrow i}^1}\mathcal{J}_E(\boldsymbol{r}_i) \tag{3}$$

provided $\Lambda_{E \leftarrow i}^1$ does not vanish, which can occur when all edges in E are bridges. Notice that it encompasses the case of any two edge currents $J_{e'}$ and J_e when E and E' have a single element each. For a simple illustration of the results, see the Appendix.

Mutual linearity does not extend straightforwardly to nonstationary currents, as can be checked by simple examples: In general, there do not exist time-dependent parameters $\lambda_{e \leftarrow i}^0(t)$ and $\lambda_{e \leftarrow i}^1(t)$ independent of $\boldsymbol{r}_i$ that would allow one to express $J_e(\boldsymbol{r}_i, t)$ as $\lambda_{e \leftarrow i}^0(t) + \lambda_{e \leftarrow i}^1(t)J_i(\boldsymbol{r}_i, t)$. To generalize to nonstationary currents we turn to the frequency domain. The probability distribution at time t is the solution $\mathbf{p}(t) = \exp(t\mathbf{R})\mathbf{p}(0)$ to the master equation, given an initial distribution $\mathbf{p}(0)$. Defining its Laplace transform $\hat{\mathbf{p}}(\varsigma) = \int_0^\infty \mathrm{d}t \, e^{-\varsigma t}\mathbf{p}(t)$ (and similarly for other functions of time), we arrive at the expression $\hat{\mathbf{p}}(\varsigma) = (\varsigma\mathbf{1} - \mathbf{R})^{-1}\mathbf{p}(0)$. Notice that both $\hat{\mathbf{p}}(\varsigma)$ and the resolvent $(\varsigma\mathbf{1} - \mathbf{R})^{-1}$ are

defined for all complex numbers not in the spectrum of $\mathbf{R}$. In that domain, this allows us to obtain closed-form expressions for the derivatives $\partial_{r_{\pm i}}\hat{j}_e(\varsigma)$ and $\partial_{r_{\pm i}}\hat{j}_i(\varsigma)$, given in Sec. IV of the Supplemental Material [19]. As in the stationary case, the important property is that their ratio $[\partial_{r_{\pm i}}\hat{j}_e(\varsigma)]/[\partial_{r_{\pm i}}\hat{j}_i(\varsigma)]$ is a constant $\hat{\lambda}^1_{e\leftarrow i}(\varsigma)$ independent of r_i, expressed as a ratio of cofactors of matrices related to the resolvent. We thus obtain

$$\hat{j}_e(\boldsymbol{r}_i,\varsigma) = \hat{\lambda}^0_{e\leftarrow i}(\varsigma) + \hat{\lambda}^1_{e\leftarrow i}(\varsigma)\hat{j}_i(\boldsymbol{r}_i,\varsigma). \tag{4}$$

This relation generalizes the stationary result Eq. (2), which is recovered in the small ς asymptotics through $\lambda^0_{e\leftarrow i} = \lim_{\varsigma\to 0}\varsigma\hat{\lambda}^0_{e\leftarrow i}(\varsigma)$ and $\lambda^1_{e\leftarrow i} = \lim_{\varsigma\to 0}\hat{\lambda}^1_{e\leftarrow i}(\varsigma)$.

Furthermore, the Laplace formalism allows us to obtain an explicit expression for $\lambda^1_{e\leftarrow i}$ in terms of sums over rooted spanning trees. We recall that in an oriented graph, a spanning tree $\mathcal{T}_{\mathsf{x}}$ with root x is a subset of edges such that every vertex of the network is connected to x via a unique path and every edge along such path points toward x. It is well-known that, up to normalization, the stationary distribution can be written as $\pi_{\mathsf{x}} \propto \tau_{\mathsf{x}}$ [18,23,24], where $\tau_{\mathsf{x}} = \sum_{\mathcal{T}_{\mathsf{x}}\subseteq\mathcal{G}} w(\mathcal{T}_{\mathsf{x}})$ is the spanning-tree polynomial, namely the sum over rooted spanning trees $\mathcal{T}_{\mathsf{x}}$ of the product $w(\mathcal{T}_{\mathsf{x}})$ of the transition rates along the tree. This result is termed the Markov chain tree theorem and is valid for arbitrary transition rates (it has been used recently [25,26] to derive bounds in such models). It is thus natural to use spanning-tree ensembles to represent the susceptibility $\lambda^1_{e\leftarrow i}$, but in this case we need to expand on these concepts. In particular, we borrow the notation \ and / from the deletion-contraction paradigm of undirected graphs. We define $\tau_{\backslash i} = \sum_{\mathsf{x}}\sum_{\mathcal{T}_{\mathsf{x}}\subseteq\mathcal{G},i\notin\mathcal{T}_{\mathsf{x}}} w(\mathcal{T}_{\mathsf{x}})$ as the sum over the subset of trees $\mathcal{T}_{\mathsf{x}}$ spanning $\mathcal{G}$ that do not contain edge i. We also define $\tau^{/i} = \sum_{\mathsf{x}}\sum_{\mathcal{T}_{\mathsf{x}}\subseteq\mathcal{G},i\subseteq\mathcal{T}_{\mathsf{x}}} w(\mathcal{T}_{\mathsf{x}}\backslash i)$ as the sum over the subset of trees $\mathcal{T}_{\mathsf{x}}$ containing edge i of the product $w(\mathcal{T}_{\mathsf{x}}\backslash i)$ of all rates but that of i. We say that edge i is, respectively, deleted or contracted in the two operations. Notice that $\tau_{\backslash i}$ and $\tau^{/i}$ are both independent of $\boldsymbol{r}_i$. Finally, we obtain the following for the susceptibility (see Sec. V of the Supplemental Material [19]):

$$\lambda^1_{e\leftarrow i} = r_{+e}\frac{\tau^{/\mathsf{s}(+e)\to\mathsf{s}(+i)}_{\backslash i,e} - \tau^{/\mathsf{s}(+e)\to\mathsf{s}(-i)}_{\backslash i,e}}{\tau_{\backslash i}}$$

$$- r_{-e}\frac{\tau^{/\mathsf{s}(-e)\to\mathsf{s}(+i)}_{\backslash i,e} - \tau^{/\mathsf{s}(-e)\to\mathsf{s}(-i)}_{\backslash i,e}}{\tau_{\backslash i}}. \tag{5}$$

Each term in the numerator of Eq. (5) corresponds to the spanning-tree polynomial of a modified network built from $\mathcal{G}$ by, first, removing edges i and e and, second, adding and contracting a directed edge from $\mathsf{s}(\pm e)$ to $\mathsf{s}(\pm i)$ (see Fig. 2 of [19] for an illustration). This means that the correct

Susceptibility

1×10^{-4} 1×10^{-3} 1×10^{-2} 1×10^{-1} 1×10^{0}
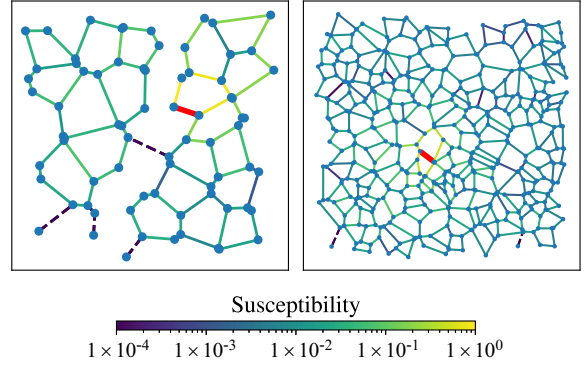
FIG. 2. Illustration of the long-range interactions between currents in multicyclic networks. We built the networks from Voronoi diagram repartitions of the plane and we randomized the rates between $1/2$ and 1. The susceptibilities are computed using Eq. (5) for every edge with respect to the input edge (thick red edge). Here, we plot the absolute value of the susceptibilities. Zero susceptibilities are represented with dashed lines and correspond to bridges. Left: the perturbation crosses the bridge and affects all the network currents. This long-range effect of single-edge perturbation is absent in detailed-balance networks. Right: the susceptibilities decrease at large distance but never vanish (except for bridges leading to leaves). The susceptibilities present a degree of heterogeneity at large distance with patches or single edges where the response is screened. See Sec. VIII of the Supplemental Material [19] for full details.

spanning-tree ensemble to compute the susceptibility is that of the original network $\mathcal{G}$ deprived of both edges e and i where one connects the vertices of the input and output edges by adding a directed edge from $\mathsf{s}(\pm e)$ to $\mathsf{s}(\pm i)$. This operation of connection is nonlocal, giving rise to long-distance interactions between currents (see Fig. 2).

The susceptibility depends on kinetic and topological properties of the process (as is the case for the bounds for state observables proven in Refs. [20,27–29]). The form of Eq. (5) implies that the susceptibility is a monotonic function of every $r_{\pm e'}$ (with $e' \neq i$) and is invariant by a global rescaling of the rates. Its extrema are thus reached by setting rates to 0 or $+1$, corresponding to "skeleton" networks that maximize or minimize the influence of the input current to the output one. In particular, notice that if i is a bridge, $\tau_{\backslash i}$ vanishes (as there are no spanning trees not containing edge i) and the susceptibility is ill-defined; in fact in that case, the input current is zero independently of r_i. Interestingly, though, Eq. (5) implies that in networks that have a bridge, the susceptibility does not vanish even when the input and output currents are on opposite sides of the bridge, despite the susceptibility (and the current) of the bridge being zero. This is due to the dependency of $\boldsymbol{\pi}$ in all the rates, out of equilibrium (see Fig. 2). Thus, Eq. (5) expresses how controlling the current of edge i builds long-distance interactions with other currents, which may be related to the overall activity [30] of the system. An additional result regarding bridges is that all currents are

strictly linear one to another (without affine coefficient) when they live on a different island than the input edge (see Sec. VI of the Supplemental Material [19]).

The Markov chain network formalism is intimately connected to the description of deterministic unimolecular chemical reaction networks (CRNs) with mass action law (see, e.g., [18,23,31–34]). A vertex $\mathsf{x} \in \mathcal{X}$ represents a chemical species A_x and an edge $e \in \mathcal{E}$ a bidirectional reaction $A_{\mathsf{s}(+e)} \rightleftarrows A_{\mathsf{s}(-e)}$ occurring at rate r_{+e} (r_{-e}) in the forward (backward) direction. The vector $\mathbf{p}(t)$ of species concentrations also evolves through $\partial_t \mathbf{p}(t) = \mathbf{R}\mathbf{p}(t)$. In such settings, which describe closed (i.e., nonchemostatted) CRNs, the results we have described so far are translated in a direct manner: the system reaches stationarity at large times, and, upon controlling J_i through r_i, output currents J_e satisfy the linearity relation Eq. (2). The sole difference is that, $\sum_\mathsf{x} p_\mathsf{x}(t)$ being conserved, the normalization of the stationary concentration $\boldsymbol{\pi}$ is fixed by its initial value $\mathbf{p}(0)$ through $\boldsymbol{\pi} \cdot \mathbf{1} = \mathbf{p}(0) \cdot \mathbf{1}$ (assumed to be independent of the rates).

We now show that the mutual linearity of currents can be extended to the case of open (i.e., chemostatted) unimolecular CRNs. To do so, we drive the system by chemostatting a subset of species $\mathsf{y} \in \mathcal{Y} \subseteq \mathcal{X}$: reservoirs create or destroy these species through reactions $\emptyset \rightleftarrows A_\mathsf{y}$, with given rates. As shown in [9], it is useful to represent such a drive by adding $|\mathcal{Y}|$ edges $f \in \mathcal{F}$, each directed from a single new vertex $\emptyset$ to a chemostatted species $\mathsf{y} = \mathsf{s}(-f)$. The stationary currents of the corresponding reactions are

$$J_f = r_{+f} - r_{-f}\pi_{\mathsf{s}(-f)}, \qquad (6)$$

where r_{+f} (r_{-f}) is the creation (destruction) rate of species $\mathsf{y} = \mathsf{s}(-f)$. Importantly, such currents are affine functions of the stationary concentration $\boldsymbol{\pi}$, in contrast to Eq. (1). The same holds for the time-dependent current, implying that the total concentration is not preserved (the dynamics is not conservative). However, one can obtain $\boldsymbol{\pi}$ by mapping the open system to a closed linear system, as follows. We consider a closed CRN on a graph of vertices $\{\emptyset\} \cup \mathcal{X}$ and edges $\mathcal{E} \cup \mathcal{F}$, and denote by $\mathbf{R}^{\mathrm{res}}$ its rate matrix. Its stationary concentration is a $(|\mathcal{X}| + 1)$-dimensional vector $\boldsymbol{\pi}^{\mathrm{res}}$ solution of $\mathbf{R}^{\mathrm{res}}\boldsymbol{\pi}^{\mathrm{res}} = \mathbf{0}$, that we normalize by imposing $\pi_\emptyset^{\mathrm{res}} = 1$. This condition, see Eq. (6), ensures that its stationary currents are identical to that of the open CRN above; by unicity, we thus have $\pi_\mathsf{x} = \pi_\mathsf{x}^{\mathrm{res}}$ for $\mathsf{x} \in \mathcal{X}$ [35]. Since the normalization $\pi_\emptyset^{\mathrm{res}} = 1$ imposes a rates-dependent constraint, the derivation of the mutual linearity has to be modified [36]. We proceed as follows: defining $\bar{\mathbf{R}}_\mathsf{x}^{\mathrm{res}}$ by replacing line x of $\mathbf{R}^{\mathrm{res}}$ by $\boldsymbol{\delta}_\emptyset \equiv (1, 0 \ldots 0)$ [placing species $\emptyset$ first], the stationarity condition $\mathbf{R}^{\mathrm{res}}\boldsymbol{\pi}^{\mathrm{res}} = \mathbf{0}$ implies $\bar{\mathbf{R}}_\mathsf{x}^{\mathrm{res}}\boldsymbol{\pi}^{\mathrm{res}} = \boldsymbol{\delta}_\mathsf{x}$ (Kronecker delta vector for vertex x). Using then the invertibility of $\bar{\mathbf{R}}_\mathsf{x}^{\mathrm{res}}$ (see Sec. II of the

Supplemental Material [19]), we express $\partial_{r_{\pm i}}\boldsymbol{\pi}^{\mathrm{res}}$ using $\bar{\mathbf{R}}_{\mathsf{s}(+i)}^{\mathrm{res}}$ and its inverse. As in the Markov chain case, this yields that the ratio $(\partial_{r_{\pm i}}J_e)/(\partial_{r_{\pm i}}J_i)$ is independent on the rates $\mathbf{r}_i$, and allows one to conclude that the mutual linearity of Eq. (2) holds for open CRNs (see Sec. III of the Supplemental Material [19] for details). Noteworthy, a chemostatting current J_f can be the input or output current (if two or more species are chemostatted, ensuring f is not a bridge).

Let us now draw conclusions and discuss open questions.

We have already seen that linearity is not a simple consequence of Kirchhoff's current law. Neither it is a straightforward consequence of the spanning-tree expression for the stationary distribution, by replacement of $\pi_{\mathsf{s}(\pm e)}$ in Eq. (1). We will explore in a forthcoming contribution some more spanning-tree combinatorics related to our main result.

The main strength of our result is that, from an operational perspective, two measurements of two currents suffice to determine $\Lambda_{E\leftarrow i}^0$ and $\Lambda_{E\leftarrow i}^1$, so further measurements have predictive power. Furthermore, the result holds in networks with more than one edge between a pair of states, and in networks with unidirectional transitions (absolute irreversibility) that typically pose a thermodynamic conundrum [37,38]. When applied to (open) resistor networks, where $r_{+e} = r_{-e}$ is the resistance of edge e, our result retrieves the "principle of superposition" of linear electric networks (see, e.g., Chap. 5 of [39]).

Although the main limitation of our result is the assumption that only the forward and backward rates of one specific transition are varied, this is met in several Markov-based biophysical models of molecular motors [40–42], conformational dynamics [43–45], DNA transcription [46], kinetic proofreading [47,48], and other processes [49,50], where rates along a single edge might be controlled by changing the concentration of a reactant chemical species (e.g., an enzyme, on the assumption of enzyme specificity). More concretely, consider an established model for the molecular motor Myosin-V [51]; perturbations in the concentration of inorganic phosphate yield a linear relation between adenosine triphosphate (ATP) consumption and the motor velocity, with affine coefficient reflecting the consumption of ATP when the motor stalls. See the Appendix for more details.

Another area of future investigation is whether the result eventually extends to population dynamics, e.g., stochastic chemical reaction networks and shot-noise electronic devices [52] where the network is potentially unbounded and the same parameter affects an infinite number of network transitions. As regards open networks of interacting units, the concept of susceptibility in interacting transport (e.g., vehicular) systems has been studied in Ref. [53].

In some physical systems, transition rates are parametrized according to local detailed balance [54,55],

e.g., $r_{+i}/r_{-i} = \exp\{\beta_i[\epsilon_{s(+i)} - \epsilon_{s(-i)}]\}$ with β_i the inverse temperature of a reservoir and ϵ_x the energy of state x. Our results apply for instance when varying β_i on a single edge. In fact, it was found that perturbing the energy of a single vertex (thus modifying the rates of all of its outward transitions) leads to a constant ratio between any currents 56]]. Another example of edge perturbation is the change of a kinetic barrier between two states.

An interesting area of overlap and future inspection is the interplay of our result with recently proposed frameworks for the composition of nonlinear chemical reaction networks [57] or of generic thermodynamic devices [58], extending concepts from linear electrical circuit theory such as that of the conductance matrix. Interestingly, however, we could not find any immediate connection of our result to the usual machinery of response theory or of large deviations, fluctuation relations, and the like. This could be an interesting area of inspection, in particular as it comes to figures of merit such as efficiency and the quality factor, which relate input and output currents to benchmark performance and allow exploration of regimes and limits of operation.

Another possibility is to use our results to make inferences about the topology and rates of the underlying network. For example, detecting nonequilibrium from available observables is relevant in many fields, in particular biophysics [59–64]. As proven in Sec. VII of the Supplemental Material [19], if the signs of susceptibilities are nonreciprocal upon swapping input and output edges, $\lambda^1_{e\leftarrow i}/\lambda^1_{i\leftarrow e} < 0$, the network is out of equilibrium (nonreciprocal edge perturbations thus require dissipation). Similarly, networks satisfying detailed balance will have zero susceptibility in all edges separated from the input by a bridge (see Sec. VI of the Supplemental Material [19]). The coefficients λ^0 and λ^1 can be empirically obtained and compared to theoretical predictions of a candidate model using Eq. (5) (or alternatively Eqs. (13) and (29) of [19]). Further inference schemes might arise from inspecting how susceptibilities change along cycles or decay with a notion of distance.

Note added—A comprehensive tutorial covering the main ideas and codes to generate the figures is available in the public repository [65].

[1] A. Einstein *et al.*, On the motion of small particles suspended in liquids at rest required by the molecular-kinetic theory of heat, Ann. Phys. (Berlin) **17**, 208 (1905).

[2] H. Nyquist, Thermal agitation of electric charge in conductors, Phys. Rev. **32**, 110 (1928).

[3] L. Onsager, Reciprocal relations in irreversible processes. I., Phys. Rev. **37**, 405 (1931).

[4] H. B. G. Casimir, On Onsager's principle of microscopic reversibility, Rev. Mod. Phys. **17**, 343 (1945).

[5] D. J. Evans, E. G. D. Cohen, and G. P. Morriss, Probability of second law violations in shearing steady states, Phys. Rev. Lett. **71**, 2401 (1993).

[6] C. Jarzynski, Nonequilibrium equality for free energy differences, Phys. Rev. Lett. **78**, 2690 (1997).

[7] M. Barbier and P. Gaspard, Microreversibility, nonequilibrium current fluctuations, and response theory, J. Phys. A **51**, 355001 (2018).

[8] D. Andrieux and P. Gaspard, A fluctuation theorem for currents and non-linear response coefficients, J. Stat. Mech. (2007) P02006.

[9] S. Dal Cengio, V. Lecomte, and M. Polettini, Geometry of nonequilibrium reaction networks, Phys. Rev. X **13**, 021040 (2023).

[10] P. Baerts, U. Basu, C. Maes, and S. Safaverdi, Frenetic origin of negative differential response, Phys. Rev. E **88**, 052109 (2013).

[11] G. Falasco, T. Cossetto, E. Penocchio, and M. Esposito, Negative differential response in chemical reactions, New J. Phys. **21**, 073005 (2019).

[12] O. Beckman, Anders Celsius and the fixed points of the Celsius scale, Eur. J. Phys. **18**, 169 (1997).

[13] E. Grodzinsky and M. Sund Levander, History of the thermometer, *Understanding Fever and Body Temperature: A Cross-disciplinary Approach to Clinical Practice* (Palgrave Macmillan, Cham, 2020), pp. 23–35.

[14] D. T. Gillespie, *Markov Processes: An Introduction for Physical Scientists* (Academic Press, Boston, 1992).

[15] N. G. v. Kampen, *Stochastic Processes in Physics and Chemistry*, 3rd ed., North-Holland Personal Library, Amsterdam (Elsevier, Boston, 2007).

[16] C. W. Gardiner, *Stochastic Methods: A Handbook for the Natural and Social Sciences*, 4th ed., Springer Series in Synergetics (Springer, Berlin, 2009).

[17] J. R. Norris and Markov chains, *No. 2 in Cambridge Series on Statistical and Probabilistic Mathematics*, 1. pbk.-ed., 15. print ed. (Cambridge University Press, Cambridge, England, 2009).

[18] J. Schnakenberg, Network theory of microscopic and macroscopic behavior of master equation systems, Rev. Mod. Phys. **48**, 571 (1976).

[19] See Supplemental Material at http://link.aps.org/supplemental/10.1103/PhysRevLett.133.047401 for technical details, proofs and additional ideas.

[20] T. Aslyamov and M. Esposito, Nonequilibrium response for Markov jump processes: Exact results and tight bounds, Phys. Rev. Lett. **132**, 037101 (2024).

[21] M. Evans and R. Blythe, Nonequilibrium dynamics in low-dimensional systems, Physica (Amsterdam) **313A**, 110 (2002).

[22] B. Altaner, M. Polettini, and M. Esposito, Fluctuation-dissipation relations far from equilibrium, Phys. Rev. Lett. **117,** 180601 (2016).

[23] T. L. Hill, Studies in irreversible thermodynamics IV. Diagrammatic representation of steady state fluxes for unimolecular systems, J. Theor. Biol. **10,** 442 (1966).

[24] F. Avanzini *et al.*, Methods and conversations in (post) modern thermodynamics, SciPost Phys. Lecture Notes 080 (2024).

[25] S. Liang, P. D. L. Rios, and D. M. Busiello, Thermodynamic bounds on symmetry breaking in linear and catalytic biochemical systems, Phys. Rev. Lett. **132,** 228402 (2024).

[26] E. Arunachalam and M. M. Lin, Information gain limit of molecular computation, arXiv:2311.15378.

[27] J. A. Owen, T. R. Gingrich, and J. M. Horowitz, Universal thermodynamic bounds on nonequilibrium response with biochemical applications, Phys. Rev. X **10,** 011066 (2020).

[28] G. Fernandes Martins and J. M. Horowitz, Topologically constrained fluctuations and thermodynamics regulate nonequilibrium response, Phys. Rev. E **108,** 044113 (2023).

[29] T. Aslyamov and M. Esposito, A general theory of static response for Markov jump processes, arXiv:2402.13990.

[30] C. Maes, Frenesy: Time-symmetric dynamical activity in nonequilibria, Phys. Rep. **850,** 1 (2020).

[31] T. L. Hill, *Free Energy Transduction and Biochemical Cycle Kinetics* (Springer, New York, NY, 1989), Vol. 1.

[32] B. L. Clarke, Stoichiometric network analysis, Cell Biophysics **12,** 237 (1988).

[33] M. Feinberg, *Foundations of Chemical Reaction Network Theory*, Applied Mathematical Sciences (Springer International Publishing, New York, 2019).

[34] R. Rao and M. Esposito, Nonequilibrium thermodynamics of chemical reaction networks: Wisdom from stochastic thermodynamics, Phys. Rev. X **6,** 041064 (2016).

[35] Notice that this implies that the stationary concentration of such open CRNs can be expressed using the Markov chain tree theorem on the rate matrix $\mathbf{R}^{\text{res}}$.

[36] The normalization $\pi_{\emptyset}^{\text{res}} = 1$ makes that $\boldsymbol{\pi}^{\text{res}} \cdot \mathbf{1}$ is different from 1 and depends generally on all the rates (as seen from the Markov Chain tree theorem). In particular we have that $\mathbf{R}_x^{\text{res}} \boldsymbol{\pi}^{\text{res}} \neq \delta_x$: $\mathbf{R}_x^{\text{res}} \boldsymbol{\pi}^{\text{res}}$ actually depends on the rates, so that the proof used in Markov Chains would not apply.

[37] Y. Murashita, K. Funo, and M. Ueda, Nonequilibrium equalities in absolutely irreversible processes, Phys. Rev. E **90,** 042110 (2014).

[38] M. Baiesi and G. Falasco, Effective estimation of entropy production with lacking data, arXiv:2305.04657.

[39] S. Seshu and N. Balabanian, *Linear Network Analysis* (Wiley, New York, 1959).

[40] V. Bierbaum and R. Lipowsky, Chemomechanical coupling and motor cycles of myosin V, Biophys. J. **100,** 1747 (2011).

[41] S. Verbrugge, L. C. Kapitein, and E. J. Peterman, Kinesin moving through the spotlight: Single-motor fluorescence microscopy with submillisecond time resolution, Biophys. J. **92,** 2536 (2007).

[42] Y. R. Chemla, J. R. Moffitt, and C. Bustamante, Exact solutions for kinetic models of macromolecular dynamics, J. Phys. Chem. B **112,** 6025 (2008).

[43] J. D. Chodera and F. Noé, Markov state models of biomolecular conformational dynamics, Curr. Opin. Struct. Biol. **25,** 135 (2014).

[44] E. Suárez, R. P. Wiewiora, C. Wehmeyer, F. Noé, J. D. Chodera, and D. M. Zuckerman, What Markov state models can and cannot do: Correlation versus path-based observables in protein-folding models, J. Chem. Theory Comput. **17,** 3119 (2021).

[45] R. D. Malmstrom, C. T. Lee, A. T. Van Wart, and R. E. Amaro, Application of molecular-dynamics based Markov state models to functional proteins, J. Chem. Theory Comput. **10,** 2648 (2014).

[46] E. A. Abbondanzieri, W. J. Greenleaf, J. W. Shaevitz, R. Landick, and S. M. Block, Direct observation of base-pair stepping by RNA polymerase, Nature (London) **438,** 460 (2005).

[47] Q. Yu, A. B. Kolomeisky, and O. A. Igoshin, The energy cost and optimal design of networks for biological discrimination, J. R. Soc. Interface **19,** 20210883 (2022).

[48] K. Banerjee, A. B. Kolomeisky, and O. A. Igoshin, Elucidating interplay of speed and accuracy in biological error correction, Proc. Natl. Acad. Sci. U.S.A. **114,** 5183 (2017).

[49] L. J. Allen, *An Introduction to Stochastic Processes with Applications to Biology* (CRC Press, Boca Raton, 2010).

[50] C. Floyd, A. R. Dinner, and S. Vaikuntanathan, Learning to control non-equilibrium dynamics using local imperfect gradients, arXiv:2404.03798.

[51] K. I. Skau, R. B. Hoyle, and M. S. Turner, A kinetic model describing the processivity of myosin-V, Biophys. J. **91,** 2475 (2006).

[52] N. Freitas, J.-C. Delvenne, and M. Esposito, Stochastic thermodynamics of nonlinear electronic circuits: A realistic framework for computing around kT, Phys. Rev. X **11,** 031064 (2021).

[53] E. Rolando and A. Bazzani, Failure detection for transport processes on networks, arXiv:2311.02624.

[54] M. Esposito, Stochastic thermodynamics under coarse graining, Phys. Rev. E **85,** 041125 (2012).

[55] G. Falasco and M. Esposito, Local detailed balance across scales: From diffusions to jump processes and beyond, Phys. Rev. E **103,** 042114 (2021).

[56] J. D. Mallory, A. B. Kolomeisky, and O. A. Igoshin, Kinetic control of stationary flux ratios for a wide range of biochemical processes, Proc. Natl. Acad. Sci. U.S.A. **117,** 8884 (2020).

[57] F. Avanzini, N. Freitas, and M. Esposito, Circuit theory for chemical reaction networks, Phys. Rev. X **13,** 021041 (2023).

[58] P. Raux, C. Goupil, and G. Verley, Circuits of thermodynamic devices in stationary non-equilibrium, arXiv:2309.12922.

[59] X. Fang, K. Kruse, T. Lu, and J. Wang, Nonequilibrium physics in biology, Rev. Mod. Phys. **91,** 045004 (2019).

[60] F. S. Gnesotto, F. Mura, J. Gladrow, and C. P. Broedersz, Broken detailed balance and non-equilibrium dynamics in living systems: A review, Rep. Prog. Phys. **81,** 066601 (2018).

[61] B. Zoller, T. Gregor, and G. Tkačik, Eukaryotic gene regulation at equilibrium, or non?, Curr. Opin. Struct. Biol. **31,** 100435 (2022).

[62] D. Hartich, A. C. Barato, and U. Seifert, Nonequilibrium sensing and its analogy to kinetic proofreading, New J. Phys. **17**, 055026 (2015).

[63] X. Yang, M. Heinemann, J. Howard, G. Huber, S. Iyer-Biswas, G. Le Treut, M. Lynch, K. L. Montooth, D. J. Needleman, S. Pigolotti, J. Rodenfels, P. Ronceray, S. Shankar, I. Tavassoly, S. Thutupalli, D. V. Titov, J. Wang, and P. J. Foster, Physical bioenergetics: Energy fluxes, budgets, and constraints in cells, Proc. Natl. Acad. Sci. U.S.A. **118**, e2026786118 (2021).

[64] P. E. Harunari, Unveiling nonequilibrium from multifilar events, arXiv:2402.00837.

[65] Pedro E. Harunari, v1.0, MutualLinearity (2024), 10.5281/zenodo.12546613.

End Matter

Appendix: Encompassing example of a simple molecular motor—To illustrate our results, we consider a Markov model that describes how the Myosin-V protein moves along an actin filament fueled by the consumption of ATP [51,56]; see Fig. 3. Each state represents a configuration of the two protein heads according to their attachment to the filament. Some transitions consume/release ATP, adenosine diphosphate, or inorganic phosphate (Pi), which is often undetected by experiments, while the flux along states 1 and 2 represents the mechanical movement. In this model, the main cycle (12345) represents the net movement of the motor, while cycle (2346) represents the futile consumption of ATP that occurs when the front head detaches and reattaches to the filament without displacement.

An analysis using Kirchhoff's current law reveals that the stationary consumption rate of ATP $\mathcal{J}_{\text{ATP}} \equiv J_{5\to1} + J_{6\to2}$ equals both the stationary release rate of adenosine diphosphate, $J_{4\to5} + J_{4\to6}$, and of Pi, $J_{\text{Pi}} \equiv J_{3\to4}$. The net movement of the protein is given by $J_{\text{m}} \equiv J_{1\to2}$ and, again due to Kirchhoff, satisfies

$$\mathcal{J}_{\text{ATP}} = J_{6\to2} + J_{\text{m}}. \tag{A1}$$

These relations hold regardless of any perturbations since they are topological constraints. We now consider changes in the environment availability of inorganic phosphate, Pi,

whose concentration enters as $r_{4\to3} \propto [\text{Pi}]$. Varying $[\text{Pi}]$ thus represents a single rate perturbation that yields a nonlinear change in all fluxes. Using our main result Eq. (2), J_{m} is found to be linearly related to the flux of Pi, $J_{\text{m}} = \lambda^0_{\text{m}\leftarrow\text{Pi}} + \lambda^1_{\text{m}\leftarrow\text{Pi}}J_{\text{Pi}}$, where we adopt the notation that $\lambda^{0,1}_{\text{m}\leftarrow\text{Pi}}$ are the coefficients related to the perturbation of $[\text{Pi}]$ that can be obtained empirically or using their analytical expressions. A similar result holds for the ATP consumption in the main cycle $J_{5\to1}$ and in the futile cycle $J_{6\to2}$.

Now, using the generalization for "macroscopic" currents Eq. (3), we find that $\mathcal{J}_{\text{ATP}}$ and J_{m} satisfy themselves a linear relation regardless of the futile consumption $J_{6\to2}$ upon perturbations of $[\text{Pi}]$:

$$\mathcal{J}_{\text{ATP}} = \lambda^0_{(5\to1)\leftarrow\text{Pi}} + \lambda^0_{(6\to2)\leftarrow\text{Pi}} - \frac{\lambda^1_{(5\to1)\leftarrow\text{Pi}} + \lambda^1_{(6\to2)\leftarrow\text{Pi}}}{\lambda^1_{\text{m}\leftarrow\text{Pi}}}\lambda^0_{\text{m}\leftarrow\text{Pi}}$$
$$+ \frac{\lambda^1_{(5\to1)\leftarrow\text{Pi}} + \lambda^1_{(6\to2)\leftarrow\text{Pi}}}{\lambda^1_{\text{m}\leftarrow\text{Pi}}}J_{\text{m}}, \tag{A2}$$

where, importantly, none of the coefficients depend on the concentration of Pi; see Fig. 3. Hence, results of the present Letter allow one to derive a relation between ATP and mechanical currents which, instead of depending on an unknown current $J_{6\to2}$ (see Eq. (A1)), is affine with coefficients that, interestingly, are independent of $[\text{Pi}]$. It establishes a direct relationship, robust to perturbations of $[\text{Pi}]$. The affine coefficient in Eq. (A2) represents the consumption of ATP when the motor stalls, which is
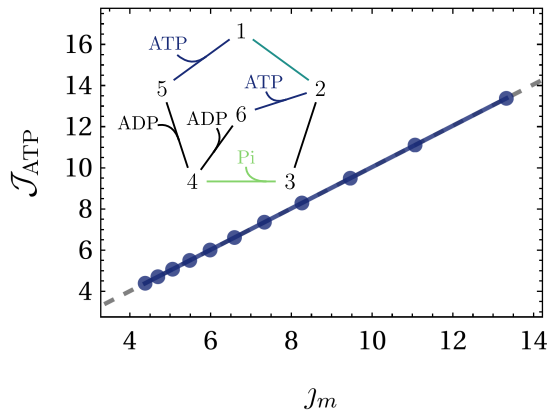

FIG. 3. Dots represent the current of ATP consumption and mechanical movement for perturbed values of $[\text{Pi}]$, the dashed gray line is obtained from Eq. (A2). Inset: network of the Myosin-V model. Further details in Sec. VIII of the Supplemental Material [19].

$$\tau^{\nearrow 5\to4}_{\searrow\{(5-1),\text{Pi}\}} = \sum_{\mathbf{x}} \sum_{\substack{\mathcal{T}_{\mathbf{x}} \subseteq \mathscr{G}^{5\to4}_{\searrow\{(5-1),\text{Pi}\}} \\ 5\to4 \subseteq \mathcal{T}_{\mathbf{x}}}} w(\mathcal{T}_{\mathbf{x}}) =$$

FIG. 4. Evaluation of $\tau^{\nearrow 5\to4}_{\searrow\{(5-1),\text{Pi}\}}$. Solid arrows represent the transition rates multiplied to form the polynomial of each tree, and the dashed arrows represent the contracted edge that is not included in the polynomial.

nonzero in our settings. Also, notice that the velocity of the motor is J_m times the step size, and is also linear with the total ATP consumption.

In this contribution, we provide more than one approach to obtain the susceptibilities involved in Eq. (A2): (i) empirically (collecting two data points of current vs current), (ii) from determinants [see Eqs. (13) and (29) of the Supplemental Material [19]], or (iii) using spanning trees [Eq. (5)]. To illustrate the latter, consider the susceptibility $\lambda^1_{(5\to1)\leftarrow\mathrm{Pi}}$. From Eq. (5), we need to evaluate the polynomials of rooted spanning trees of modified networks, one of them is $\tau^{/5\to4}_{\backslash(5-1),\mathrm{Pi}}$, which corresponds to the spanning trees of the original network deprived of the input edge $\mathrm{Pi} = (3-4)$ and from the output edge $(5-1)$, and including the connecting edge $5\to4$. All the rooted spanning trees of this network with the contraction of $5\to4$ are represented in Fig. 4.

An analysis of the coefficients' numerical values is also informative. Using the experimentally motivated transition rates described in [56], we find that the affine part of Eq. (A2) is 8×10^{-11}, while the susceptibility is 1.005. It tells that the rates were selected so that the futile consumption of ATP is small and most ATP consumption is directly transformed into movement.